frontiers | Frontiers in Earth Science

TYPE Original Research
PUBLISHED 09 April 2024
DOI 10.3389/feart.2024.1393211

OPEN ACCESS

EDITED BY
Xixin Wang,
Yangtze University, China

REVIEWED BY
Xianguo Zhang,
China University of Petroleum, China
Wenjie Feng,
Yangtze University, China
Gang Hui,
University of Calgary, Canada

*CORRESPONDENCE
Youjing Wang,
wangyoujing@petrochina.com.cn

RECEIVED 28 February 2024
ACCEPTED 26 March 2024
PUBLISHED 09 April 2024

CITATION
Qi Y, Wang Y, Qin G, Song Y, Zhang H and Meng F (2024), Sedimentary evolutionary processes, architecture, and sedimentary model of a lobate shallow-water delta: insights from flume simulation experiments. *Front. Earth Sci.* 12:1393211. doi: 10.3389/feart.2024.1393211

Sedimentary evolutionary processes, architecture, and sedimentary model of a lobate shallow-water delta: insights from flume simulation experiments

You Qi, Youjing Wang*, Guosheng Qin, Yanchen Song, Hualing Zhang and Fanle Meng

PetroChina Research Institute of Petroleum Exploration and Development, Beijing, China

By using equipment such as time-lapse cameras and 3D laser scanners, this study conducted flume simulation experiments to obtain topographic elevation, the amount of sediment increment, sedimentary cross sections, and other related data and diagrams. Quantitative software was then utilized for sedimentological analysis to clarify the depositional evolution, architecture, and depositional model of lobate shallow-water deltas. The research results show that under the influence of hydraulic conditions and main distributary channels, lobate shallow-water deltas primarily undergo three evolution stages: initial channel formation, distributary channel system formation, and continuous stable evolution stage. The architecture elements of lobate shallow-water deltas can be divided into distributary channels dominated by channel deposition, proximal river mouth bars, transitional bars, and distal bars. The lateral composition and downstream deposition of the river-bar combination are the main structural units of the shallow water delta. The proximal profile distributary channels exist in the form of thick channel sand bodies with multiple repetitive intercalation cycles, and thick proximal bar deposits form on both sides of the distributary channels. The bifurcation of distributary channels in the middle profile leads to a reduction in channel scale, while large-scale proximal bars still develop on both sides of the channel. In the distal profile, a substantial river mouth bar complex is formed at the break of the delta front slope, and with the gradual progradation of the delta, the river mouth bar deposition zone becomes flattened. Based on the insights of the flume simulation experiments, a sedimentary model for lobate shallow-water delta was established.

KEYWORDS

lobate delta, flume experiments, evolution processes, architecture, sedimentary model

1 Introduction

Fisk et al. (1954,1961) first proposed the concept of shallow-water deltas in the study of the Mississippi River Delta. Subsequent scholars, through comprehensive research in delta formation dynamics, lithological characteristics, and other areas

(Hoy and Ridgway, 2003; Olariu and Bhattacharya, 2006), have summarized the geological background for the formation of lacustrine shallow-water deltas. It is characterized by its formation in gently sloping, slowly subsiding depression basins, with relatively shallow water and a stable tectonic backdrop, forming deltas within plateaus and continental shelves, distinct from typical Gilbert-type deltas.

Shallow-water deltaic depositional systems have been successively discovered in multiple continental basins in China, including the Songliao Basin (Zhu et al., 2012; Deng et al., 2015; Hu et al., 2015), Bohai Bay Basin (Zhu et al., 2008; Xu et al., 2019), Ordos Basin (Liu et al., 2011; Chen et al., 2023), and many modern lakes such as the Poyang Lake. The shallow-water delta is divided into delta plain subfacies, delta front subfacies, and pro-delta subfacies. Using the shallow-water delta in the Sanzhao Depression of the Songliao Basin as an example, Zhu Xiaomin (Zhu et al., 2012) suggested that the webbed deltaic depositional front facies developed under humid climate conditions, with a broad front facies zone that can be divided into inner and outer fronts. Zhang (2010) used modern sedimentation in Poyang Lake as a reference and proposed that distributary channel-type deltas with lobate and lobe-shaped skeletal sand bodies and delta plain sedimentation are well developed, occupying over 3/4 of the delta area, while the delta front facies zone is relatively less developed. Fu et al. (2021) and Chen et al. (2021) analyzed the application of seismic sedimentology in subfacies division of shallow-water deltas and the identification of distributary channel sand bodies. Wang et al. (2020) and Qin et al. (2020) respectively discussed the classification of distributary channel sedimentation models and the sedimentary characteristics and models of front tabular sand in shallow-water deltas. In the Ordos Basin, Li et al. (2019), Liu et al. (2021) and Zhu et al. (2021) conducted comprehensive analyses of shallow-water delta reservoir lithological characteristics, sand body distribution patterns, and front mouth bar deposition characteristics in the Yanchang Formation. Shallow-water deltas have been classified based on different source systems, control factors, and sand body morphologies (Heerden and Roberts, 1988; Lemons and Chan, 1999; Longhitano, 2008; Nagy et al., 2010; Zhang et al., 2010; Cahoon et al., 2011; Yin et al., 2012; Zhu et al., 2013; Yin et al., 2014; Wu et al., 2019). Sand body morphology is a relatively direct classification method, dividing shallow-water deltas into tabular, lobate, braided, and bird's foot types based on sand body distribution patterns. Among them, lobate shallow-water deltas often have a large plan-view scale and longitudinally rich sand body development and have been found to be ideal reservoirs among several billion-ton scale oilfields globally, making them a very important type of shallow-water delta.

With the advancement of computer technology, geomorphological measurements, and recording techniques (Woodward et al., 2003; Feng et al., 2011; Qiao et al., 2015; Zeng et al., 2017b), flume simulation experiments have gradually become a reliable means of sedimentological research (Zeng C. et al., 2017; Bai et al., 2018; Wei et al., 2020; Wang et al., 2023). Scholars initiated flume simulation experiments as early as the 1960s (McKee, 1957). Compared to studies based on geological outcrops and modern sedimentation (Zhang, 1996; Jia et al., 2000; Jiao et al., 2005), their primary advantage lies in the convenience of measurements (easily slice and sample), detailed recording of sedimentary processes, and the significant implications for sedimentological research and determining the general distribution patterns of reservoirs. Flume simulation experiments can provide a large amount of sand body model parameters at different sedimentary stages, and can more intuitively and three-dimensionally depict the sedimentation process.

The Triassic Yanchang Formation in the Yishan Slope of the Ordos Basin, China, has gentle structural slopes with dips of less than 1 and a stable distribution of stratum thickness (Fu et al., 2017). It is divided into ten sand groups from bottom to top, undergoing complete cyclical changes from lake transgression to regression. Among these, the Chang 6 sand group develops thick oil-rich lobate shallow-water deltaic front sand bodies, which are the main reservoir units (Figure 1). In the middle to late stages of development, a finer characterization of the internal configuration of sand bodies is necessary to correspond to later oilfield development, given the complex and intricate sedimentary interfaces within lobate shallow-water deltas. Advanced experimental and analytical methods are urgently required to clarify the sedimentary evolution of this type of delta and to better identify its internal structural characteristics. Taking the Chang 6 lobate delta in the Wuliwan area of the Jing'an Oilfield in the Yishan Slope of the Ordos Basin as an example, this study sets parameters including sediment grain size, hydraulic conditions, and slope gradient similar to those underground to simulate the evolution of the shallow-water delta in the research area through flume experiments, dissect its internal configuration characteristics, establish a sedimentary model, and provide guidance for water flooding adjustments in the oilfield.

2 Experimental design and methodology

2.1 Experimental device design

The shallow-water delta simulation device consists of a bedform, water supply unit, sand supply unit, water level-controlled boundary, and laser scanner, etc. (Figure 2). Previous flume simulation experiments used sandy platforms as the bedform to simulate a flat basin (lv, 2020). In order to simulate the sedimentary evolution of the shallow-water delta as accurately as possible and to replicate its sediment characteristics, this simulation device features a different bed shape design compared to previous shallow-water delta flume experiments. The design of the base of the simulated region is characterized by a plain-slope-break-front style to better observe the evolution processes of the delta distributary channels and to focus on researching the bar combinations of the shallow-water delta. The slope of the base is set at 0.55° in accordance with the ancient slope of underground reservoirs. The length of the delta plain sedimentary area is 2.9 m, which matches the ancient sedimentary conditions of the reservoir's long gentle slope and short lake area. On the plan view, the slope-break area serves as the boundary, reflecting the sedimentary characteristics of the delta plain subfacies from the source area to the slope-break area, and the sedimentary characteristics of the pro-delta subfacies from the slope-break area to the boundary.

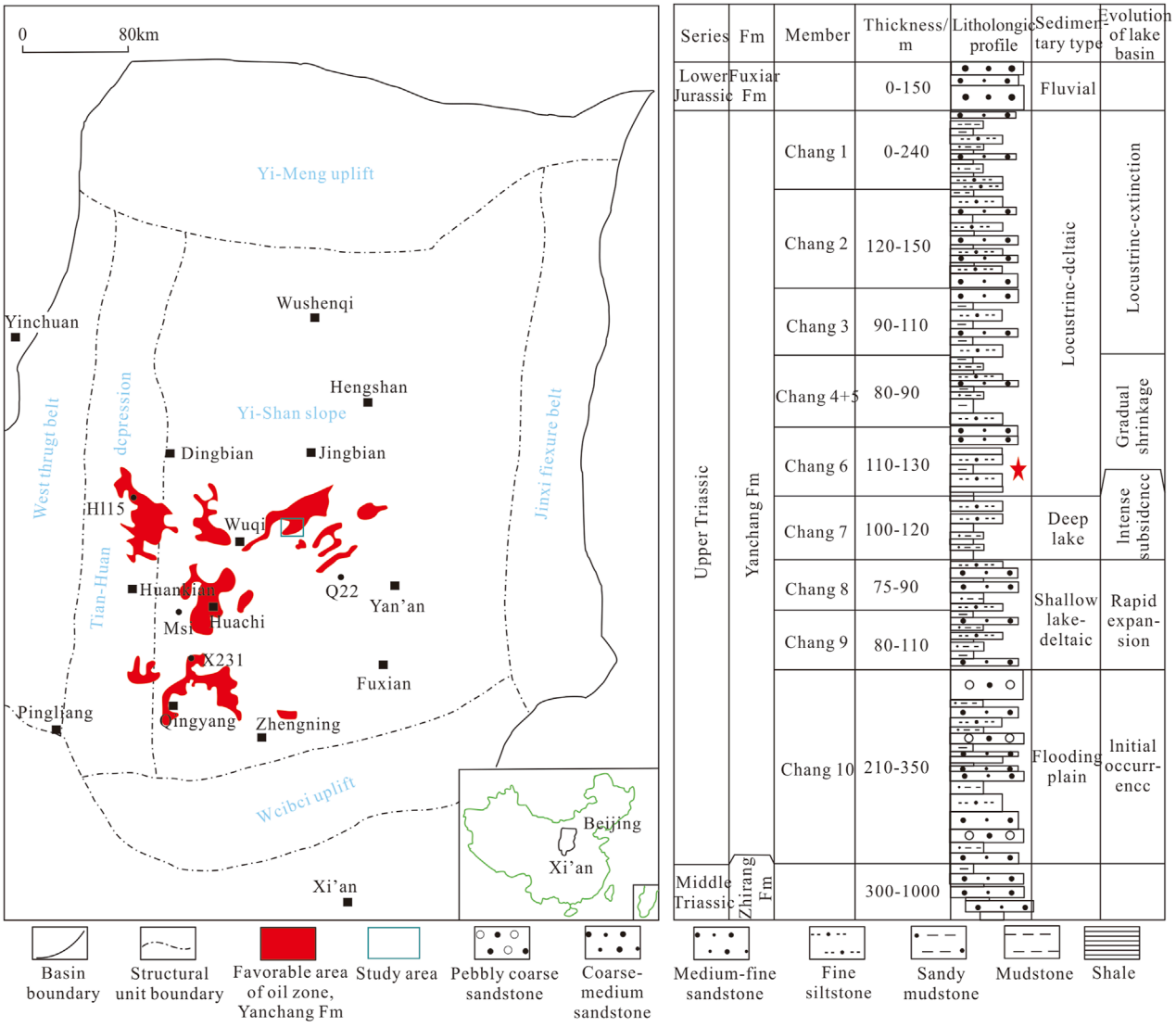

FIGURE 1
Comprehensive histogram of the location and stratigraphy of the study area modified based on Fu et al. (2017).

In the downstream, a water level control boundary was set to maintain the stability of the water level. Additionally, a constant-speed water pump was placed in the water body of the delta front deposition area as the experimental water supply device to ensure stable water conditions through a circulated water supply. In order to obtain images and topography information during the sedimentary evolution of the shallow-water delta, a time-lapse photography device was installed above the flume setup to capture real-time image information during the sedimentary evolution process. Furthermore, one spatial reference information collection point (alignment point) and 4 laser scanning stations were set up. After each period, the sedimentary area was scanned using the FARO-S70 laser scanner to obtain sub-millimeter laser scans for three-dimensional coordinates, images, and terrain topography records of the sedimentary bodies.

During the flume simulation process, in order to ensure accurate measurement of sedimentary terrain topography by the laser scanner, the simulation was conducted in cycles of 60 min/120 min, after the water was stopped and drained at the end of each cycle, the laser scanning was performed to avoid measurement errors caused by water refraction.

2.2 Preparation of simulation parameters

Based on the experimental analysis results of Chang 6 reservoir and the outcrop of the Yanchang Formation in the Wuliwan area of the Jing'an Oilfield in the Ordos Basin, and regarding similar international experiment parameters and sediment numerical simulation parameter values, experimental parameters such as the slope of the base, sediment composition, water flow velocity and discharge, sand supply, and water viscosity were determined using a proportional reduction method (Table 1).

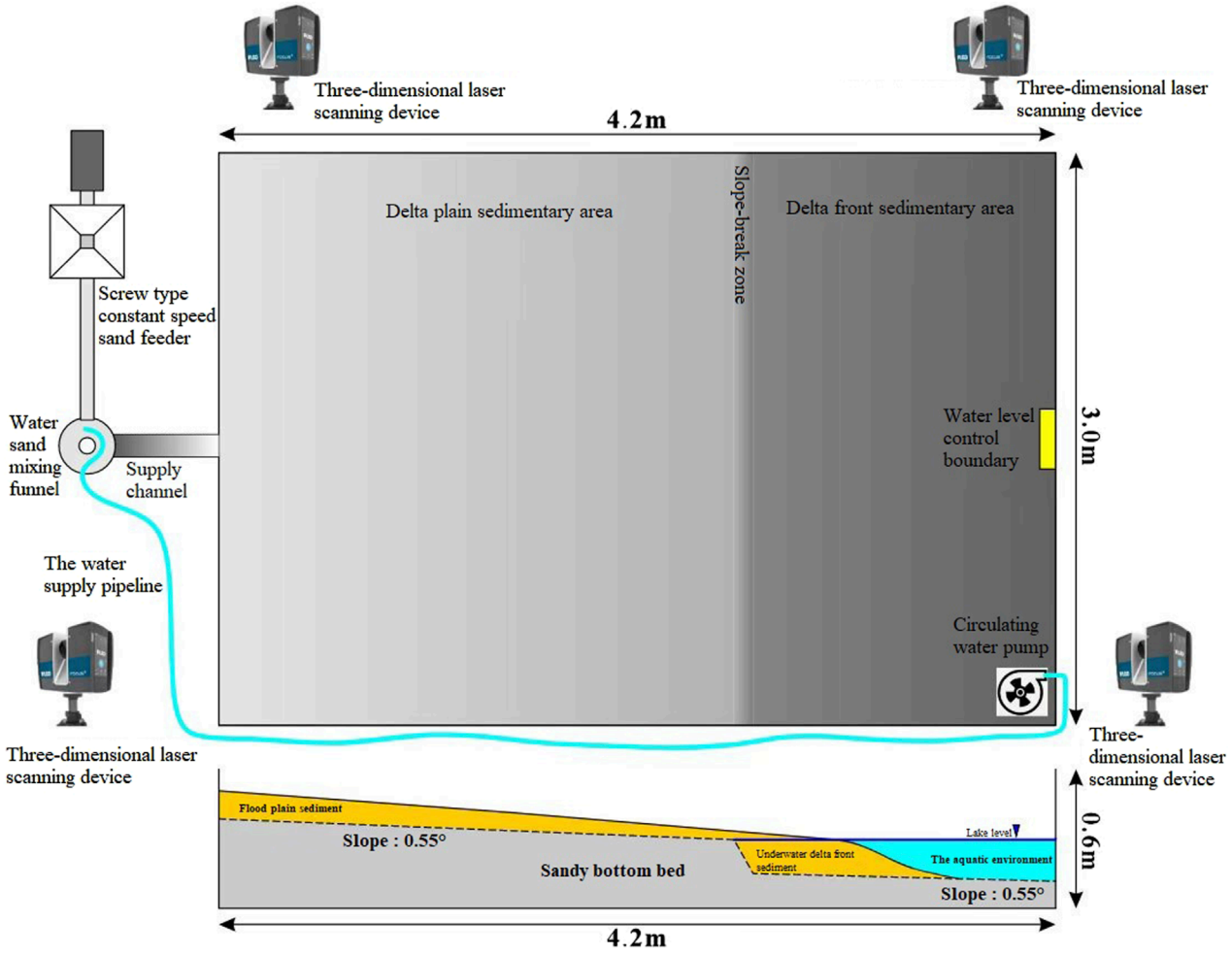

FIGURE 2
Schematic diagram of the flume simulation experiment facility.

2.3 Simulation data processing

The 138-h experiment was monitored throughout the process. After the completion of the simulation experiment, real-time image information of the sediment evolution process recorded by the time-lapse photography equipment can be obtained. The three-dimensional spatial information calculation and alignment were conducted using SCENE software for the point cloud data generated from each simulation period regarding the coordinates of the reference collection point. Utilizing the QuantSedAnaV2.0 programming software, the aligned billion-level three-dimensional point cloud data were gridded, and operations such as outlier handling and image correction were performed. After data gridding, error analysis and data volume correction were carried out. Measurement error trends were obtained based on the calibration objects at the edges of the experimental setup, and the data volume was corrected for errors in each period to obtain the simulated data volume of the experiment. The experimental data volume includes coordinates, grid numbers, simulation periods, elevation, image information, etc., and can generate topographic elevation maps, sediment increment maps, and cross-sections for further analysis of the sediment evolution process.

3 Analysis of experimental results

3.1 Sedimentary evolution process during each stage

The experiment recorded the evolving orthophoto images (Figure 3), de-trended topographic maps (Figure 4), and the sedimentation thickness increment within a specified observation timeframe (Figure 5) (positive values representing sedimentation, negative values representing erosion). De-trending helped eliminate the influence of long-profile elevation differences and primarily reflected the geomorphology of the delta.

In the laboratory flume simulation, the initial bed was a gently sloping sandy layer to simulate a relatively flat terrain before the formation of a shallow-water delta. The evolution of the lobate shallow-water delta from nonexistence to stability evolution

10.3389/feart.2024.1393211

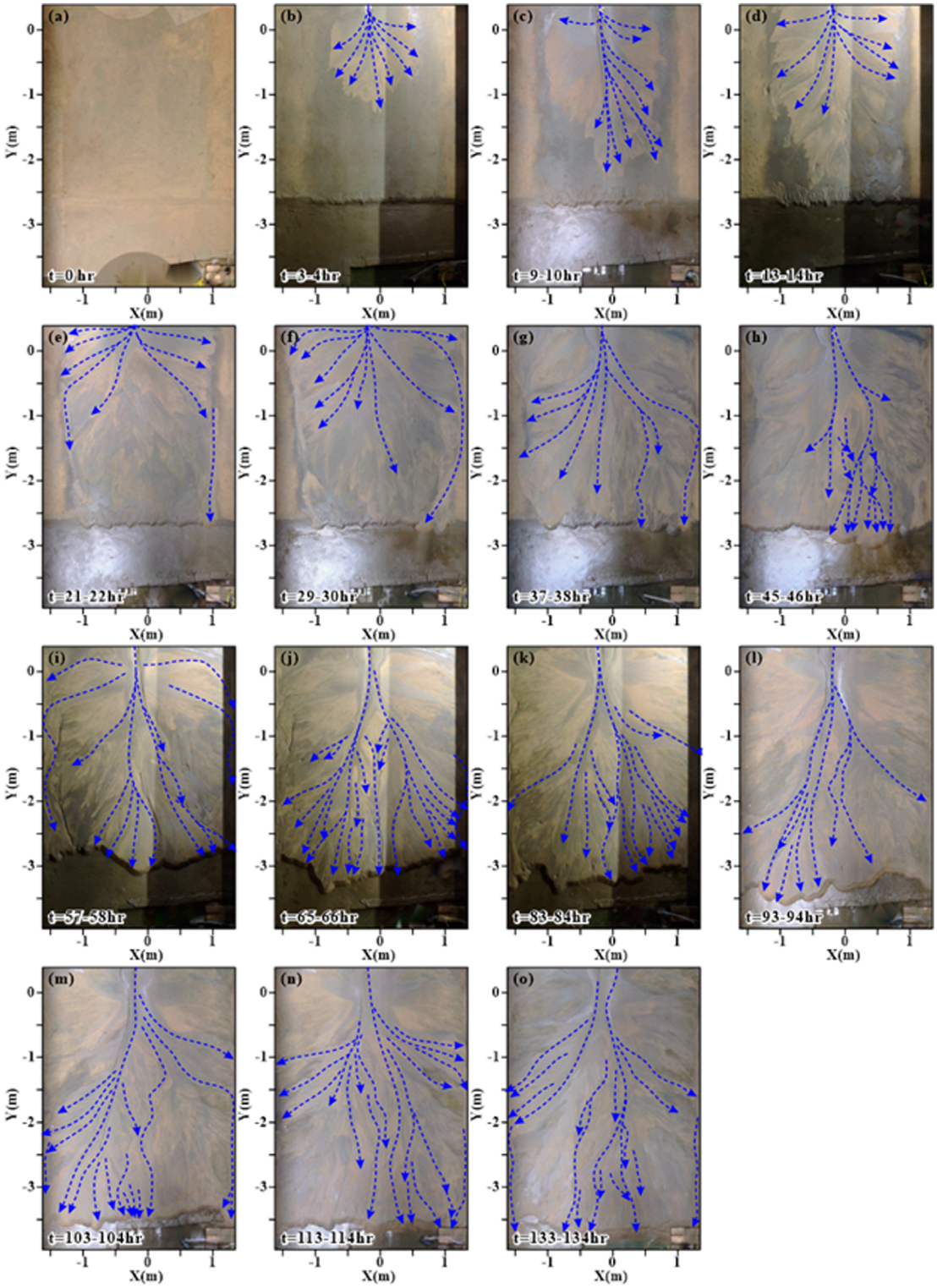

FIGURE 3
Orthorectified image of the evolution of the lobate-shaped shallow water delta in the simulation of the flume experiment. Blue dashed lines indicated the flow path during each simulation period. **(A)** Experiment time: 0 hour; **(B)** Experiment time: 3-4 hours; **(C)** Experiment time: 9-10 hours; **(D)** Experiment time: 13-14 hours; **(E)** Experiment time: 21-22 hours; **(F)** Experiment time: 29-30 hours; **(G)** Experiment time: 37-38 hours; **(H)** Experiment time: 45-46 hours; **(I)** Experiment time: 57-58 hours; **(J)** Experiment time: 65-66 hours; **(K)** Experiment time: 83-84 hours; **(L)** Experiment time: 93-94 hours; **(M)** Experiment time: 103-104 hours; **(N)** Experiment time: 113-114 hours; **(O)** Experiment time: 133-134 hours.

10.3389/feart.2024.1393211

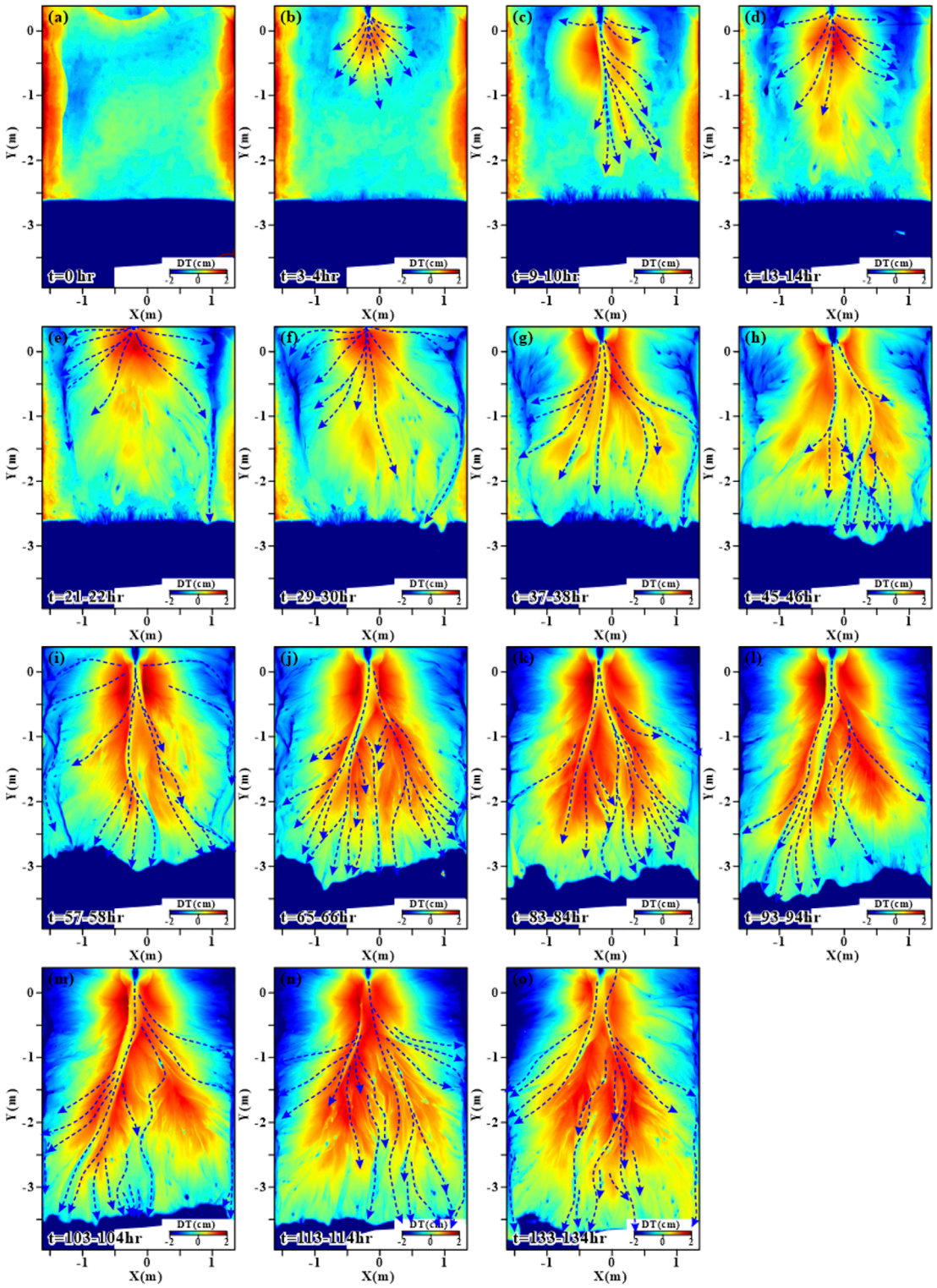

FIGURE 4
Topographic map (downstream trend was de-trended) of the lobate-shaped shallow water delta in the simulation. Blue dashed lines indicated the flow path during each simulation period. **(A)** Experiment time: 0 hour; **(B)** Experiment time: 3-4 hours; **(C)** Experiment time: 9-10 hours; **(D)** Experiment time: 13-14 hours; **(E)** Experiment time: 21-22 hours; **(F)** Experiment time: 29-30 hours; **(G)** Experiment time: 37-38 hours; **(H)** Experiment time: 45-46 hours; **(I)** Experiment time: 57-58 hours; **(J)** Experiment time: 65-66 hours; **(K)** Experiment time: 83-84 hours; **(L)** Experiment time: 93-94 hours; **(M)** Experiment time: 103-104 hours; **(N)** Experiment time: 113-114 hours; **(O)** Experiment time: 133-134 hours.

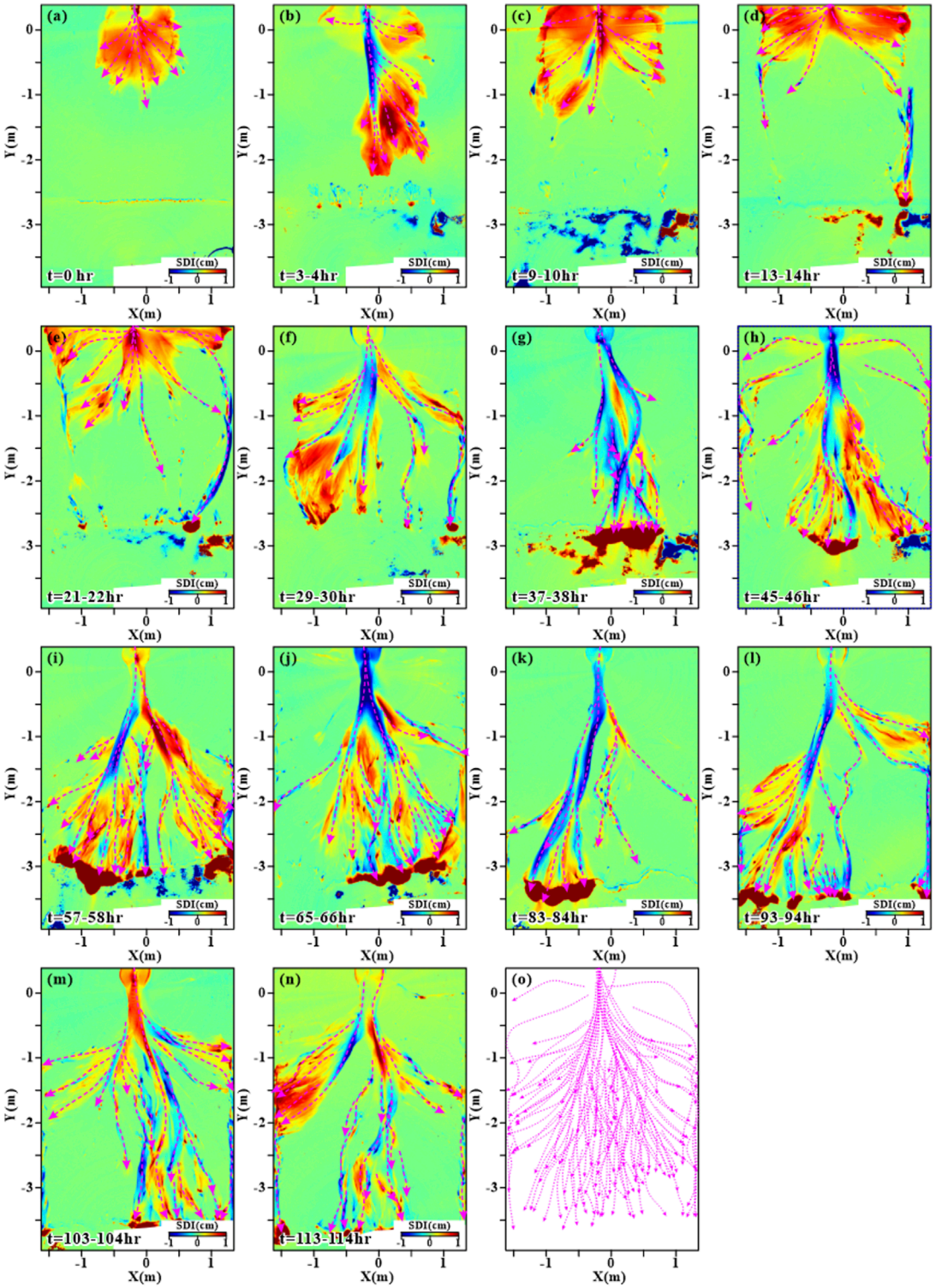

FIGURE 5
Sediment thickness increment for each run step. A value greater than 0 indicates that sedimentation has occurred within one run step, with an increase in sedimentation thickness. If the value is less than 0, it means that erosion has occurred within one simulation period, and the sediment thickness has decreased. Magenta dashed lines indicated the flow path during each simulation period. **(A)** Experiment time: 0 hour; **(B)** Experiment time: 3-4 hours; **(C)** Experiment time: 9-10 hours; **(D)** Experiment time: 13-14 hours; **(E)** Experiment time: 21-22 hours; **(F)** Experiment time: 29-30 hours; **(G)** Experiment time: 37-38 hours; **(H)** Experiment time: 45-46 hours; **(I)** Experiment time: 57-58 hours; **(J)** Experiment time: 65-66 hours; **(K)** Experiment time: 83-84 hours; **(L)** Experiment time: 93-94 hours; **(M)** Experiment time: 103-104 hours; **(N)** Experiment time: 113-114 hours; **(O)** mainstream line distribution.

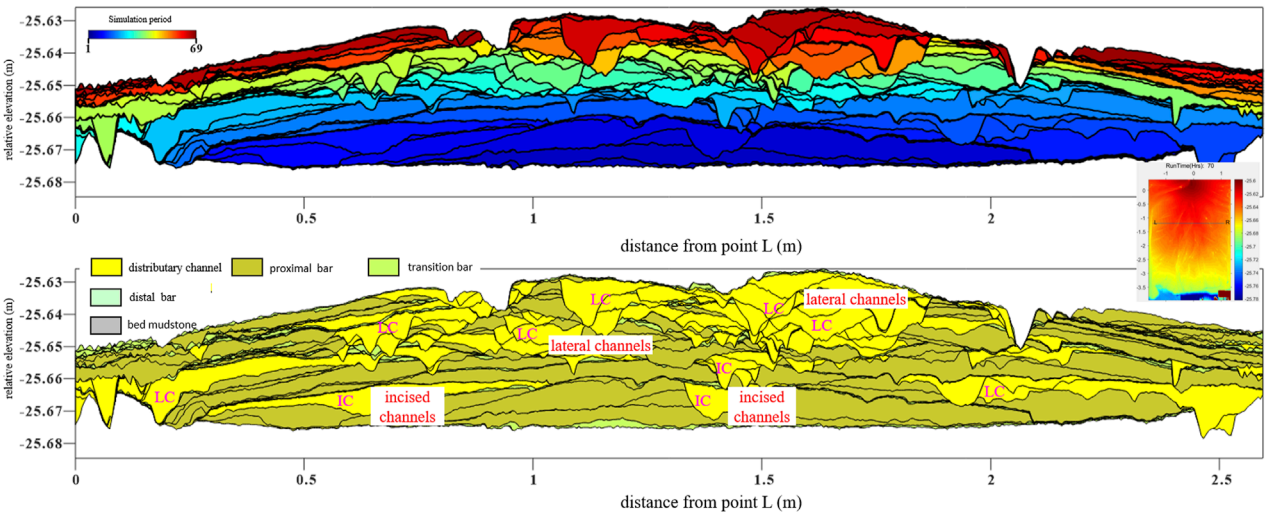

FIGURE 6
Sedimentary architecture of the experimental delta at the upstream part. The upper figure was the reproduced strata based on the topography data. The bottom figure was the sedimentary architecture interpreted based on the upper figure. LC means the lateral migration channel; IC means the incised channel.

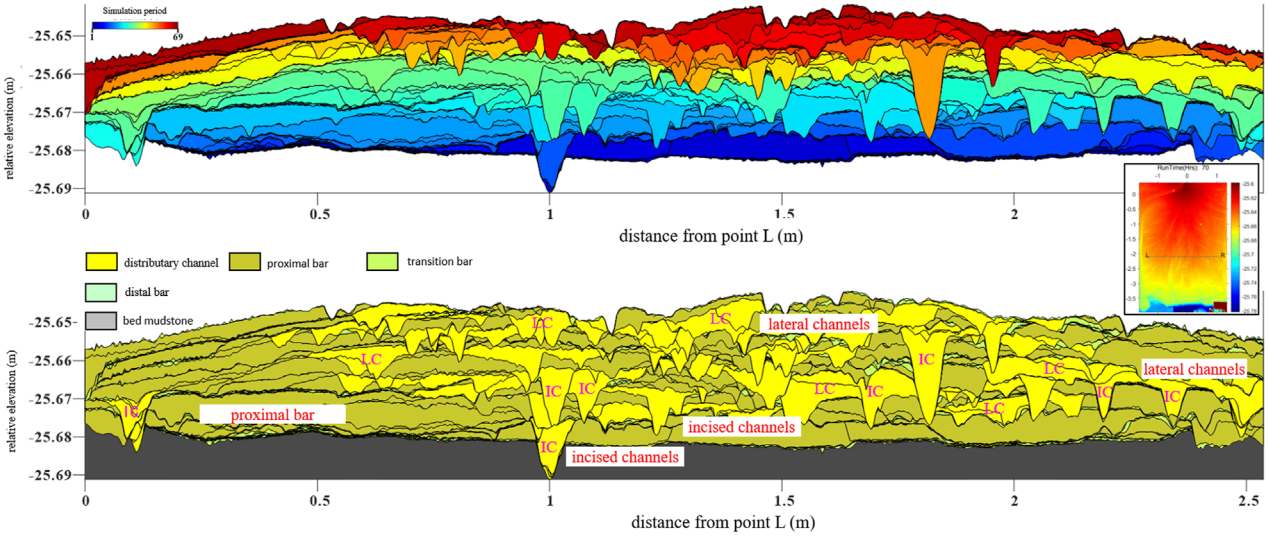

FIGURE 7
Sedimentary architecture of the experimental delta at the middle part. The upper figure was the reproduced strata based on the topography data. The bottom figure was the sedimentary architecture interpreted based on the upper figure. LC means the lateral migration channel; IC means the incised channel.

mainly underwent three stages: the initial channel formation stage, distributary channel system formation stage, and continuous stable evolution stage.

3.1.1 Initial channel formation stage

In the early stages of the sediment simulation (Figures 3A–D, 4A–D), sediment primarily developed in the plain region. As the simulated river entered the water body, the expansion of water flow resulted in a decrease in flow velocity due to the top support effect. With the decrease in river energy, some immobile sediment was unloaded in the river mouth area. Gradually, this resulted in the formation of subaqueous shoals due to the deposition of bedload sediments from the river, which gradually increased in height, forming river mouth sand bars. The obstruction by the river mouth sand bars led to the branching of the original single river channel, forming initial distributary channels. These initial distributary channels then formed secondary river mouth sand bars, leading to further channel bifurcation

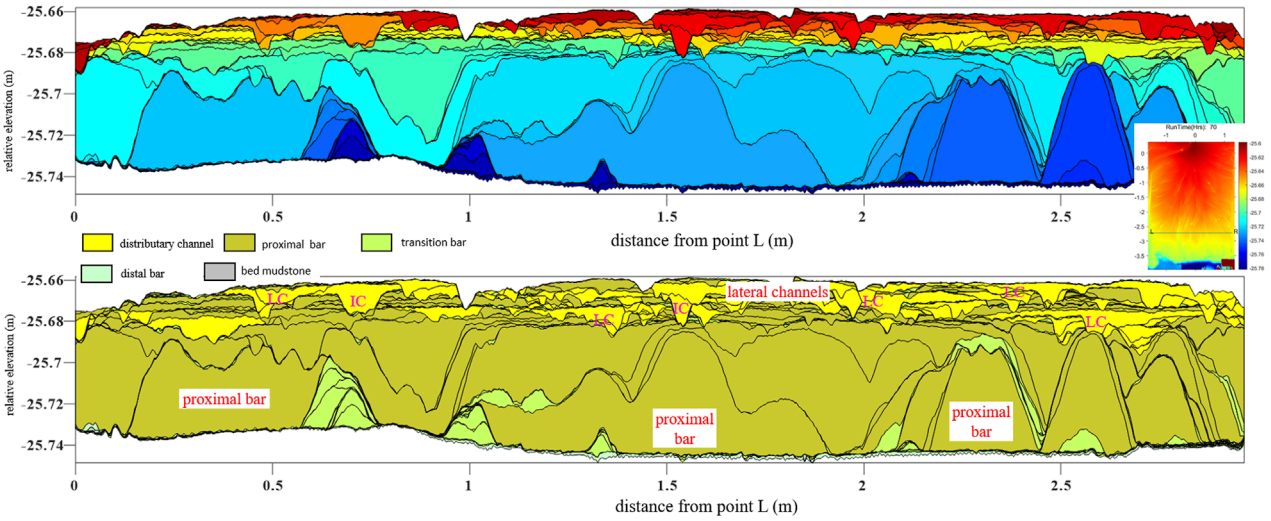

FIGURE 8
Sedimentary architecture of the experimental delta at the distal part. The upper figure was the reproduced strata based on the topography data. The bottom figure was the sedimentary architecture interpreted based on the upper figure. LC means the lateral migration channel; IC means the incised channel.

and the formation of the initial shape of the lobate shallow-water delta.

3.1.2 Distributary channel system formation

After a period of continuous evolution (Figures 3E–H, 4E–H), the delta area expanded gradually, the number of distributary channels increased, and under the constraint of various rank estuarine sand bars, the delta extended downstream. This included the development of wider, deeply incising main distributary channels, as well as narrower, frequently meandering distributary channels. The main and distributary channels together formed the river network system on the delta surface, which gradually became more complex as the delta continued to grow.

3.1.3 Continuous stable evolution stage

Under sustained water flow and sediment supply, the delta continued to evolve (Figures 3I–O, 4I–O). Distributary channels further migrated, evolved, and amalgamated, and after nearly a hundred simulation cycles, the delta area was stabilized. The growth of the delta's edges slowed down, while the distributary channels on its surface migrated rapidly and frequently, leading to further rapid changes in the relationship between distributary channels and river mouth bars. However, during this period, the overall sedimentary characteristics of the delta remained stable.

3.2 Sedimentary architecture patterns

Based on high-precision experimental geomorphological laser scanning data and comprehensive sediment simulation experiments, each period of the experimental flume simulation results was de-trended to highlight the morphological and distribution characteristics of channels and sandbars and to conduct architecture dissection. With an increase in the number of experiments, the delta on the plain gradually transformed from a simple pattern of deltaic forms into a complex architecture of compound deltaic-estuarine systems. On the cross-section, sediment deposition evolved from simple vertical stacking to a more complex structure due to channel erosion.

3.2.1 Basic configuration unit combination

The morphological units of a lobate-shaped shallow water delta can be divided into distributary channels dominated by river sediment, proximal river mouth bars, transitional bars, and distal bars. A typical lobate-shaped shallow water delta is mainly composed of large-scale multi-branched deltaic-estuarine systems, which gradually grow in size as they extend towards the water body. Throughout the entire sedimentary evolution of the shallow water delta, the sediment characteristics of the deltaic-estuarine systems display different features at various stages of the experiment:

Initial channel formation stage: During this stage (Figures 5A–D), sediment deposition is primarily incremental and fans out in the plain region around the river mouth. The channels exhibit low sinuosity and experience rapid sediment filling. A small number of the channels have incision capabilities (Figure 5B). Overall, the distribution of the channels and river mouth bars is relatively concentrated. The river mouth bars mainly distribute on both sides of the initial channel and secondary distributary channels, with minimal incision caused by the channels.

Distributary channel system formation stage: At this stage (Figures 5E–H), although the delta continues to grow, the rate of growth is slower than it was in the initial stage. The erosive capacity of the channels increases, with two types of erosion observed: incision and lateral cutting due to the lateral migration of the river, forming migrating side-cut channels. Both types of channels coexist during this stage. The river mouth bars formed in the previous stage increase in size and extend towards the distal end. As the distributary channels extend forward and enter

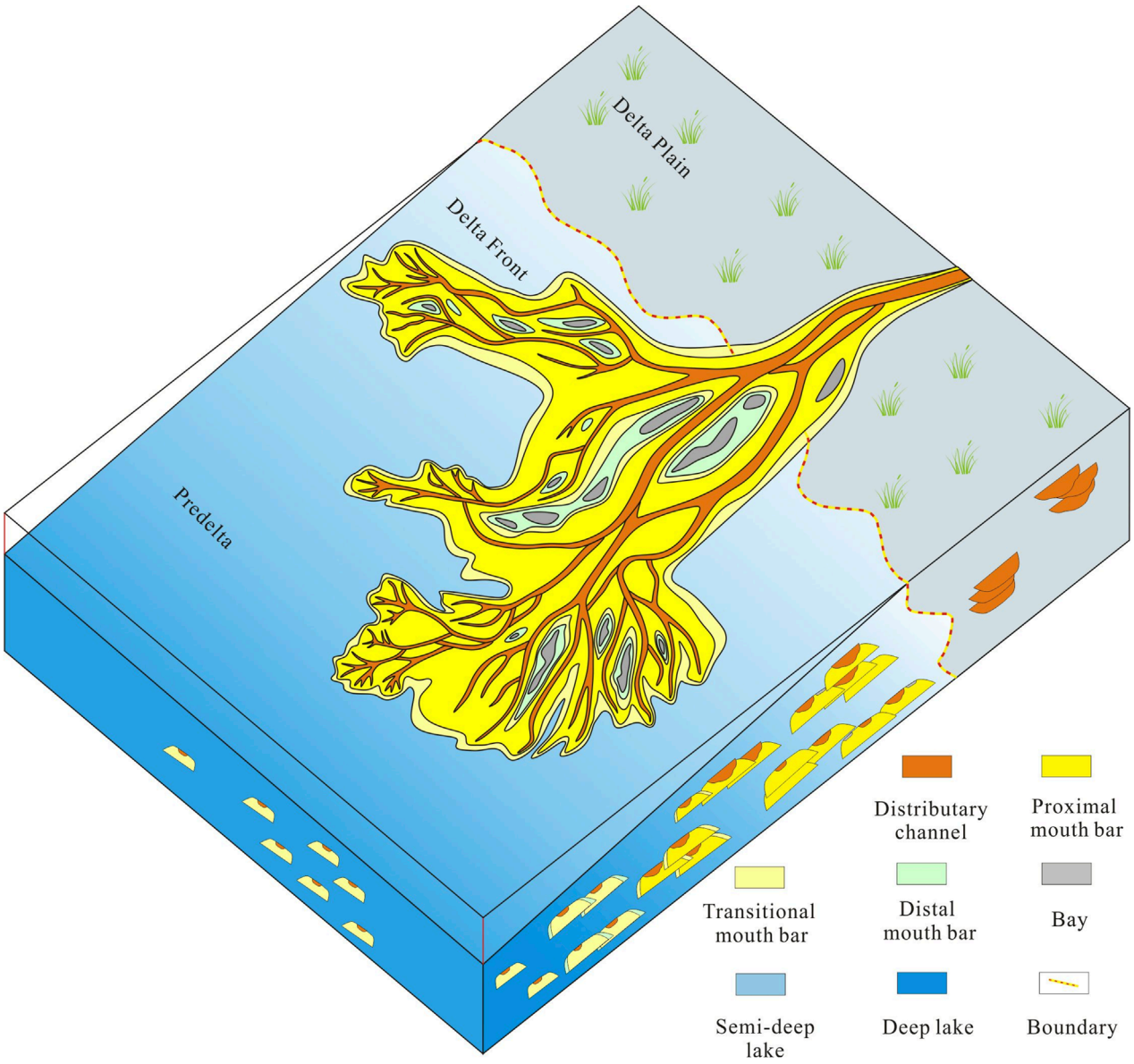

FIGURE 9
Sedimentary model of the Triassic Yanchang Formation Chang 6 Sand Formation in Jing'an Oilfield, Yishan Slope, Ordos Basin.

deeper water bodies, the hydrodynamic force decreases rapidly, resulting in the formation of distal bars at the termination of the channels (Figures 5G, I, J).

Continuous stable evolution stage: In this stage (Figures 5I–N), due to continuous water flow and sediment supply, the delta development gradually stabilizes, with a slow increase in area. The incision effect of the channels becomes more pronounced. As the distributary channels gradually extend forward and the river network (Figure 5O) becomes more complex, the cutting effect of the channels becomes more apparent. The stability of the distal channel system is lower than that of the proximal channel system, with a prevalence of migrating side-cut channels. The distribution of previously deposited river mouth bars becomes more complex due to the influence of the changing network of the river systems, and together with the distributary channel deposit end bars that extend continuously, formed the multiple fringe-shaped river mouth bar combinations. Under a stable sedimentation background, the delta system exhibits periodic cycles of progradation and retrogradation.

3.2.2 Proximal depositional configuration

The proximal cross-sectional profile is selected from sediment deposits close to the source in the upper plain (Figure 6), distributary channels often exist in the form of multi-period repetitive and overlapping wide-banded thick-layer channel sand bodies, with thick deposits of proximal bars formed on both sides of the distributary channels. Under a stable tectonic and sediment supply background, the delta progrades continuously, transitioning from front-edge deposition to plain deposition from bottom to top. The plain distributary channels

TABLE 1 Parameter settings for flume simulation experiments.

Sedimentary conditions	Jing'an Oilfield Wuliwan District Chang6	Experimental parameters
Paleoslope	0.5°–0.6°	0.55°(3.5 cm/5 m)
Lithology	Fine sandstone dominated	Fine sand dominated
Sediment fraction	Medium sand, fine sand, silt, mud	10% medium sand, 50% fine sand, 20% silt, 20% mud
Supply channel	Large main-stem distributary channel	Large main-stem distributary channel (braided river)
Hydrodynamic conditions	Strong hydrodynamic, high sandy supply	Water supply: 0.4 L/s sand supply 4 g/s
Sand transport rate	High	10 kg/m3
Water-sediment cohesion	Lower	Lower (clean water + suspended sediment)
Basin structure	Long gentle slopes + short lakes	Long gentle slopes + short lakes
Evolutionary processes	Combination of reciprocating, overlapping, and reverse prosodic progressions	Multiple phases of incoming sedimentation
Main phenomena	Widespread distributary channel, complex overlapping incision	Frequent overlapping and cutting evolution of distributary channels
Experimental period	None	2 h/period × 69 periods

mainly include incised channels (IC) and lateral cut channels (LC). The development of distributary channels gradually increases, transitioning from isolated to lateral stacking pattern, while the development and continuity of river mouth bars reduce progressively.

3.2.3 Mid-range depositional configuration

The mid-range cross-sectional profile is located in the upper zone of the entire shallow water delta-front deposit (Figure 7), and the sedimentation shifts from delta-front edge deposits to plain deposits from bottom to top. The development of distributary channels gradually increases, transitioning from isolated channels into laterally stacked ones, while the development and continuity of river mouth bars decrease gradually. The distributary channels still exhibit lateral stacking migration but at a significantly smaller scale compared to the upstream profile, indicating that the branching of the distributary channels results in a smaller channel scale. Large-scale proximal bars continue to develop on both sides of the channels, and these proximal bars are often incised by other distributary channels, leading to the presence of multiple distributary channels within a single proximal bar. Compared to the proximal cross-sectional profile, the scale of the bar combinations decreases, while the number of depositional periods increases in the mid-range cross-sectional profile.

3.2.4 Distal deposition configuration styles

The distal profile is located in delta fronts because most sediment develops underwater (Figure 8), and it shows the formation of large-scale river mouth bar complexes at the sediment slope break near the delta front, generally distributed in the lower part of the profile. As the delta gradually progrades, the river mouth bar deposition rapidly transitions into a plain. Even after plain formation, deltaic sedimentation still develops bar combinations, although the scale of these bar combinations is relatively smaller compared to the proximal profile. Along the front slope break zone, thick river mouth bar complexes are developed at the base, with lateral high stacking forming extensive interconnected thick river mouth bars and bodies. Delta progradation leads to their top plain formation, resulting in laterally amalgamated thin sand layers. The development of distributary channels in the plain sedimentation layer increases from bottom to top, with enhanced stacking. In the distal portion, distributary channels primarily migrate laterally, with lower incision depth.

We have highlighted the new insights from the experimental delta. Firstly, the distributary channels dominated the deposition and evolution. For a distributary channel, its upper reach is incised into the previously deposited sediments, and transported the sediments to its distal reach to form channel mouth bars. Therefore, the sedimentary architecture of the finally preserved experimental delta was complicated by the migration and avulsion of the distributary channels.

Secondly, the channel mouth bars were cut and transformed by the later distributary channels, the preservation of channel mouth bars, especially for the proximal bars were poorly preserved in the experimental delta."

3.3 Sedimentary model

Based on the identification of configuration units, a clear combination pattern between different configuration units was established through a detailed interpretation of multiple typical

cross-sectional profiles. The main channels are mostly isolated within extensively developed floodplains, with nearly no contact with other configuration units. Distributary channels, proximal river mouth bars, transitional bars, and distal bars are the primary configuration units at the delta front. The combination pattern of river mouth bar configuration units is complex, with the potential for self-stacking to form different types of river mouth bar complexes. Additionally, river mouth bars can combine with distributary channels to form various patterns, with the most common being the downcutting of distributary channels into the lower deposited river mouth bars.

Based on the above understanding, a sedimentary configuration model for the Triassic Yanchang Formation Chang 6 Sand Formation in Jing'an Oilfield, Yishan Slope, Ordos Basin was established (Figure 9). Based on changes in the lake basin water level, the overall sedimentary environment can be divided into delta plains, delta fronts, and pre-deltas from the land towards the lake basin direction. The delta plain can be further divided into upper and lower plains. The main sedimentary configuration unit evolves from the upper plain backbone channel to the lower plain distributary channel and ultimately to the delta front river mouth bars. Distributary channels and river mouth bars are the main genetic sand bodies, with distributary channels often showing lateral migration and superposition along with remodeling the early river mouth bars, ultimately leading to the development of thick layers of sand bodies.

4 Conclusion

Based on flume simulation experiments, the sedimentary process of a lobate shallow-water delta mainly goes through three evolutionary stages: initial channel formation, distributary channel system formation, and continuous stable evolution stage. The configuration units of the lobate shallow-water deltas can be divided into distributary channels, proximal river mouth bars, transitional bars, and distal bars. Lateral amalgamation of bar complexes and progradation are the main structural units of the shallow water deltas. During the continuous growth of the delta, distributary channels extend forward gradually, and the river network becomes more complex. Multiple fringe-like river mouth bar combinations can be formed at the delta front.

In the proximal profile, distributary channels often exist in the form of multiple stages of repeated overlapping thick channel sandbodies, while thick proximal bar deposition forms on both sides of the distributary channels. In the mid-range profile, the sedimentation changes from front-end deposition to plain deposition from bottom to top. The development of distributary channels gradually increases, and the channels shift from isolated to lateral superposition. The development and continuity of river mouth bars gradually decrease. In the distal profile, a large-scale river mouth bar complex is observed at the sediment slope break at the distal end of the delta front, distributed in the lower part of the profile. However, as the delta gradually progrades, the river mouth bar deposition area becomes a plain. Based on the identification of configuration units and the systematic interpretation of typical profiles, a sedimentary model of the Triassic Yanchang Formation Chang 6 Sand Formation in Jing'an Oilfield, Yishan Slope, Ordos Basin was established.

Data availability statement

The original contributions presented in the study are included in the article/Supplementary material, further inquiries can be directed to the corresponding author.

Author contributions

YQ: Conceptualization, Formal Analysis, Resources, Writing–original draft. YW: Conceptualization, Funding acquisition, Project administration, Supervision, Visualization, Writing–review and editing. GQ: Data curation, Methodology, Writing–original draft. YS: Investigation, Writing–review and editing. HZ: Validation, Writing–review and editing. FM: Validation, Writing–review and editing.

Funding

The author(s) declare that financial support was received for the research, authorship, and/or publication of this article. This research was funded by "Research and demonstration of key technologies of ballast engineering in mature oil fields of PetroChina," grant number 2023YQX10201.

Acknowledgments

The authors gratefully acknowledge the comments from reviewers and the academic editors for their constructive reviews of the manuscript.

Conflict of interest

The authors declare that the research was conducted in the absence of any commercial or financial relationships that could be construed as a potential conflict of interest.

Publisher's note

References

Bai, Y. C., Hu, X., Xu, H. Y., Zou, D. S., and Bai, Y. (2018). Experimental simulation analysis of shallow water delta formation process in lake. *J. Hydraulic Eng.* 49 (05), 549–560. doi:10.13243/j.cnki.slxb.20171157

Cahoon, D. R., White, D. A., and Lynch, J. C. (2011). Sediment infilling and wetland formation dynamics in an active crevasse splay of the Mississippi River delta. *Geomorphology* 131 (3-4), 57–68. doi:10.1016/j.geomorph.2010.12.002

Chen, C., Qi, Y., Yu, Z. L., and Wang, B. (2021). Seismic identification of channel sand body superposition in shallow water delta: a case study of Linxing S area, eastern Ordos Basin. *Nat. Gas. Geosci.* 32 (5). doi:10.11764/j.issn.1672-1926.2021.02.003

Chen, X., Xiao, L., Wang, M. Y., Hao, C. X., Wang, F., and Tang, H. N. (2023). Provenance and palaeo-sedimentary environment restoration of Chang 8 oil-bearing Formation in southwestern margin of Ordos Basin: evidence from rock geochemistry. *Curr. Geol.* 37 (05), 1264–1281. doi:10.19657/j.geoscience.1000-8527.2023.037

Deng, Q. J., Hu, M. Y., Hu, Z. G., and Wu, Y. K. (2015). Sequence stratigraphic framework and sedimentary system distribution of Fuyu oil layer in Shuangcheng area, northern Songliao Basin. *Curr. Geol.* 29 (03), 609–622. doi:10.3969/j.issn.1000-8527.2015.03.013

Feng, X., Zou, L. L., Liu, C., Lu, Q., Liang, W. J., Li, L. L., et al. (2011). Forward modeling of fully polarimetric GPR. *J. Geophys. Eng.* 54 (2), 349–357. doi:10.3969/j.issn.0001-5733.2011.02.011

Fisk, H. N. (1961). *Bar-finger sands of Mississippi delta*. New York, NY, USA: Springer.

Fisk, H. N., Kolb, C. R., McFarlan, E., and Wilbert, L. J. (1954). Sedimentary framework of the modern Mississippi delta [Louisiana]. *J. Sediment. Res.* 24 (2), 76–99. doi:10.1306/d4269661-2b26-11d7-8648000102c1865d

Fu, J., Deng, X., Wang, Q., Li, J., Qiu, J., Hao, L., et al. (2017). Densification and hydrocarbon accumulation of triassic Yanchang Formation Chang 8 member, Ordos Basin, NW China: evidence from geochemistry and fluid inclusions. *Petroleum Explor. Dev.* 44 (1), 48–57. doi:10.1016/s1876-3804(17)30007-1

Fu, X., Du, X. F., Guan, D. Y., Li, J., and Li, X. H. (2021). Application of seismosedimentology to the study of sedimentary facies of river-shallow water delta: a case study of guantao Formation in penglai A structure area, Bohai sea. *Bull. Geol. Sci. Technol.* 40 (3), 96–108. doi:10.19509/j.cnki.dzkq.2021.0304

Heerden, I. L. V., and Roberts, H. H. (1988). Facies development of Atchafalaya delta, Louisiana: a modern bayhead delta. *Aapg Bull.* 72. doi:10.1306/703c8eb1-1707-11d7-8645000102c1865d

Hoy, R. G., and Ridgway, K. D. (2003). Sedimentology and sequence stratigraphy of fan-delta and river-delta deposystems, Pennsylvanian Minturn Formation, Colorado. *Aapg Bull.* 87 (7), 1169–1191. doi:10.1306/03110300127

Hu, M. Y., Sun, C. Y., Xue, D., and Zhang, H. J. (2015). High resolution sequence study of the 4th member of the quansi Formation in the Sanzhao area, northern Songliao. *Curr. Geol.* 29 (04), 765–776. doi:10.3969/j.issn.1000-8527.2015.04.006

Jia, A. L., Mu, L. X., Chen, L., and Huang, S. Y. (2000). Fine research method of fan delta reservoir outcrop. *J. Petroleum Sci. Eng.* 43 (04), 105–108+125.

Jiao, Y., Yan, J., I, S. L., Yang, R., Lang, F., and Yang, S. (2005). Architectural units and heterogeneity of channel reservoirs in the Karamay Formation, outcrop area of Karamay oil field, Junggar basin, northwest China. *Aapg Bull.* 89 (4), 529–545. doi:10.1306/10040400955

Lemons, D. R., and Chan, M. A. (1999). Facies architecture and sequence stratigraphy of fine-grained lacustrine deltas along the eastern margin of late Pleistocene Lake Bonneville, northern Utah and southern Idaho. *AAPG Bull.* 83 (4), 635–665. doi:10.1306/00aa9c14-1730-11d7-8645000102c1865d

Li, Y., Zhang, Y. F., Wang, T., Zhang, Q., Wang, M., Li, R. Z., et al. (2019). Sedimentary facies of Chang 1 member of upper triassic Yanchang Formation and development law of shallow delta mouth bar in zizhou area, Ordos Basin. *J. Palaeogeogr.* 21 (5), 757–766. doi:10.7605/gdlxb.2019.05.051

Liu, H. L., Qiu, Z., Xu, L. M., Qin, W. F., Tong, Q., Lin, J. H., et al. (2021). Distribution of shallow water delta sand bodies and the genesis of thick layer sand bodies of the Triassic Yanchang Formation, Longdong Area, Ordos Basin. *PETROLEUM Explor. Dev.* 48 (1), 123–135. doi:10.1016/s1876-3804(21)60009-5

Liu, H. Q., Li, X. B., Wan, Y. R., Wei, L. H., and Liao, J. B. (2011). Paleogeographic environment and sedimentary characteristics of Chang 8 reservoir Formation in Ordos Basin. *J. Sediment. Res.* 29 (06), 1086–1095. doi:10.14027/j.cnki.cjxb.2011.06.005

Longhitano, S. G. (2008). Sedimentary facies and sequence stratigraphy of coarse-grained gilbert-type deltas within the pliocene thrust-top potenza basin (southern apennines, Italy). *Sediment. Geol.* 210 (3-4), 87–110. doi:10.1016/j.sedgeo.2008.07.004

Lv, J. L., Zhu, Y. J., Xia, R., Zheng, Y. K., Liu, C. H., Feng, W. J., et al. (2020). Sedimentary characteristics and evolution process of arid branch river system: experimental study of flume sedimentation simulation. *J. Sediment. Res.* 38 (05), 994–1005. doi:10.14027/j.issn.1000-0550.2019.101

McKee, E. D. (1957). Flume experiments on the production of stratification and cross-stratification. *J. Sediment. Res.* 27 (2), 129–134. doi:10.1306/74d70678-2b21-11d7-8648000102c1865d

Nagy, J., Hess, S., and Alve, E. (2010). Environmental significance of foraminiferal assemblages dominated by small-sized Ammodiscus and Trochammina in Triassic and Jurassic delta-influenced deposits. *Earth-Science Rev.* 99 (1-2), 31–49. doi:10.1016/j.earscirev.2010.02.002

Olariu, C., and Bhattacharya, J. P. (2006). Terminal distributary channels and delta front architecture of river-dominated delta systems. *J. Sediment. Res.* 76 (2), 212–233. doi:10.2110/jsr.2006.026

Qiao, H., Wang, Z. Z., Li, L., Li, H. M., Pan, L., and Wang, K. Y. (2015). The establishment of a knowledge base on meandering river geology using satellite imagery and its practical applications. *Curr. Geol.* 29 (6), 1444. doi:10.3969/j.issn.1000-8527.2015.06.020

Qin, R. S., Yue, H. L., Zhou, F. J., Wu, Q. Y., and Lei, Y. (2020). Sedimentary characteristics and models of the ribbon sand in the foreland of a river-controlled shallow water delta: a case study of the lower ming member in block 34 of bozhong area, yellow river mouth sag. *Acta Sedimentol. Sin.* 38 (2). doi:10.14027/j.issn.1000-0550.2019.027

Wang, X., Wei, S. Y., Lu, Q. Q., Dai, R., Hu, H., Bi, Y. H., et al. (2023). Development process and formation mechanism of transverse sand bar in delta front based on physical simulation. *J. Sediment. Res.* 41 (03), 818–827. doi:10.14027/j.issn.1000-0550.2021.150

Wang, X. B., Jiang, Z. X., Hu, G. Y., Fan, T. E., Fan, H. J., He, M. W., et al. (2020). Classification of sedimentary patterns of distributary channels in shallow water deltas. *J. Earth Sci. Environ.* 42 (5). doi:10.19814/j.jese.2020.04053

Wei, S. Y., Liu, Z. B., Wu, S. H., and Wang, X. T. (2020). Simulation experiments on alluvial fan sedimentation process and sedimentary configuration controlled by normal faults. *J. Palaeogeogr.* 22 (06), 1095–1108. doi:10.7605/gdlxb.2020.06.074

Woodward, J., Ashworth, P. J., Best, J. L., Sambrook Smith, G. H., and Simpson, C. J. (2003). The use and application of GPR in sandy fluvial environments: methodological considerations. *Geol. Soc. Lond. Spec. Publ.* 211 (1), 127–142. doi:10.1144/gsl.sp.2001.211.01.11

Wu, S. H., Xu, Z. H., and Liu, Z. (2019). river-controlled shallow water delta sedimentary architecture. *J. Palaeogeogr.* 21 (02), 202–215.

Xu, Z., Wu, S., Liu, Z., Zhao, J., Geng, H., Wu, J., et al.(2019). Configuration characteristics of finger sand bars in shallow water delta front: a case study of the lower member of Neogene Minghuazhen Formation in Bohai BZ25 oilfield, Bohai Bay Basin. *PETROLEUM Explor. Dev.* 46(02), 322–333. doi:10.11698/PED.2019.02.12

Yin, T. J., Li, X. Y., Zhang, C. M., Zhu, Y. J., and Gong, F. H. (2012). Morphological characteristics of sedimentary sandbodies in modern shallow lake basin deltas: a case study of dongting lake and Poyang Lake. *J. Petroleum Nat. Gas Technol.* 34 (10), 1–7+166. doi:10.3969/j.issn.1000-9752.2012.10.001

Yin, T. J., Zhang, C. M., Zhu, Y. J., Yang, W., Ye, J. G., Cai, W., et al. (2014). A special type of shallow delta–the superimposed delta. *J. Geol.* 88 (02), 263–272. doi:10.19762/j.cnki.dizhixuebao.2014.02.009

Zeng, C., Yin, T. J., and Song, Y. K. (2017a). Numerical simulation experiment of sedimentation of shallow water delta under lake level rise and fall. *Earth Sci.* 42 (11), 2095–2104. doi:10.3799/dqkx.2017.134

Zeng, Q. L., Zhang, R. H., lu, W. Z., Wang, B., and Wang, C. Y. (2017b). Study on the development law and controlling factors of fractures based on 3D laser scanning technology: a case study of the outcrop profile of suohan village in kuqa foreland area, tarim basin. *Nat. Gas. Geosci.* 28 (3). doi:10.11764/j.issn.1672-1926.2017.02.004

Zhang, C. M. (2010). Shallow water delta sedimentary model. *J. Sediment. Res.* 28 (5), 933–944. doi:10.14027/j.cnki.cjxb.2010.05.006

Zhang, C. M., Xu, L., Lin, K. X., Liu, H. B., and Qiu, Y. N. (1996). The anatomical study of the distributary channel sands in the 68th layer of the Oil Sand Mountain oilfield in Qinghai. *J. Sediment. Res.* 55 (04), 71–77.

Zhang, C. M., Yin, T. J., Zhu, Y. J., and Ke, L. M. (2010). Shallow water delta sedimentary model. *J. Sediment. Res.* 28 (05), 933–944. doi:10.14027/j.cnki.cjxb.2010.05.006

Zhu, S. F., Cui, H., Chen, J. H., Luo, G. J., Wang, W. Y., Yang, Y., et al. (2021). Sedimentary system and reservoir petrology of shallow water delta–A case study of the 8th member of the Shan 1 yihe Formation in the western Ordos Basin. *Acta Sedimentol. Sin.* 39 (1). doi:10.14027/j.issn.1000-0550.2020.115

Zhu, W. L., Li, J. P., Zhou, X. H., and Guo, Y. H. (2008). Neogene shallow water delta sedimentary system and large oil and gas field exploration in Bohai Sea. *J. Sediment. Res.* 48 (04), 575–582.

Zhu, X. M., Liu, Y., Fang, Q., Li, Y., Liu, Y. Y., Wang, R., et al. (2012). Formation conditions and sedimentary model of shallow water delta in large depression lacustrine basin: a case study of Fuyu oil reservoir in Sanzhao sag, Songliao Basin. *Front. earth Sci.* 19 (01), 89–99.

Zhu, X. M., Pan, R., Zhao, D. N., Liu, F., Wu, D., Li, Y., et al. (2013). Formation and development of shallow water delta in lake basin and case analysis. *J. China Univ. Petroleum Nat. Sci. Ed.* 37 (05), 7–14. doi:10.3969/j.issn.1673-5005.2013.05.002